









RESEARCH ARTICLE | JUNE 01 2023

Disordering two-dimensional magnet-particle configurations using bidispersity

K. Tsuchikusa; K. Yamamoto ; M. Katsura; C. T. de Paula ; J. A. C. Modesto ; S. Dorbolo ; F. Pacheco-Vázquez ; Y. D. Sobral ; H. Katsuragi  



J. Chem. Phys. 158, 214501 (2023)

<https://doi.org/10.1063/5.0149803>



View
Online



Export
Citation

CrossMark

Articles You May Be Interested In

Structural and viscous properties of bidispersed magnetic colloids

AIP Conference Proceedings (April 2014)

Rotation dynamics and internal structure of self-assembled binary paramagnetic colloidal clusters

J. Chem. Phys. (October 2021)

Phase coexistence in a polydisperse charged hard-sphere fluid: Polymer mean spherical approximation

J. Chem. Phys. (September 2005)

500 kHz or 8.5 GHz?
And all the ranges in between.

Lock-in Amplifiers for your periodic signal measurements



Find out more

 Zurich
Instruments

Disordering two-dimensional magnet-particle configurations using bidispersity

Cite as: J. Chem. Phys. 158, 214501 (2023); doi: 10.1063/5.0149803

Submitted: 8 March 2023 • Accepted: 8 May 2023 •

Published Online: 1 June 2023



View Online



Export Citation



CrossMark

K. Tsuchikusa,¹ K. Yamamoto,^{1,2}  M. Katsura,¹ C. T. de Paula,³  J. A. C. Modesto,³  S. Dorbolo,⁴ 
F. Pacheco-Vázquez,⁵  Y. D. Sobral,³  and H. Katsuragi^{1,a)} 

AFFILIATIONS

¹Department of Earth and Space Science, Osaka University, 1-1 Machikaneyama, Toyonaka 560-0043, Japan

²Water Frontier Research Center (WaTUS), Tokyo University of Science, 6-3-1 Niijuku, Katsushika-ku, Tokyo 125-8585, Japan

³Departamento de Matemática, Universidade de Brasília, Campus Universitário Darcy Ribeiro, Brasília, DF 70910-900, Brazil

⁴GRASP, Institute of Physics, Building B5a, Sart Tilman, Université de Liège, B4000 Liège, Belgium

⁵Instituto de Física, Benemérita Universidad Autónoma de Puebla, Apartado Postal J-48, 72570 Puebla, Mexico

^{a)}Author to whom correspondence should be addressed: katsuragi@ess.sci.osaka-u.ac.jp

ABSTRACT

In various types of many-particle systems, bidispersity is frequently used to avoid spontaneous ordering in particle configurations. In this study, the relation between bidispersity and disorder degree of particle configurations is investigated. By using magnetic dipole–dipole interaction, magnet particles are dispersed in a two-dimensional cell without any physical contact between them. In this magnetic system, bidispersity is introduced by mixing large and small magnets. Then, the particle system is compressed to produce a uniform particle configuration. The compressed particle configuration is analyzed by using Voronoi tessellation for evaluating the disorder degree, which strongly depends on bidispersity. Specifically, the standard deviation and skewness of the Voronoi cell area distribution are measured. As a result, we find that the peak of standard deviation is observed when the numbers of large and small particles are almost identical. Although the skewness shows a non-monotonic behavior, a zero skewness state (symmetric distribution) can be achieved when the numbers of large and small particles are identical. In this ideally random (disordered) state, the ratio between pentagonal, hexagonal, and heptagonal Voronoi cells becomes roughly identical, while hexagons are dominant under monodisperse (ordered) conditions. The relation between Voronoi cell analysis and the global bond orientational order parameter is also discussed.

Published under an exclusive license by AIP Publishing. <https://doi.org/10.1063/5.0149803>

I. INTRODUCTION

When modeling the behaviors of many-particle systems, a monodisperse system usually results in an ordered structure. However, most of the natural particle systems exhibit a random particle configuration, in general. To achieve a random particle configuration, two types of particles (usually large and small) are mixed as a bidisperse system. In a previous study,¹ the relation between bidispersity and particle configuration was investigated through the ordering of force chain orientations using the photoelastic effect, which allows for a direct access to the force chain network. According to their result, the order parameter of the force-chain orientational order becomes roughly constant within the range of 10%–90% bidispersity [defined as the ratio of the area occupied by small (large)

disks to the total area of the disks]. This result suggests that even a 10% bidispersity is adequate to generate random particle configurations. It is important to note, however, that the randomness of the force chain structure and particle configuration may not coincide. The preceding investigation solely examined the force-chain orientational order. To properly characterize the particle configuration order in detail, we should directly measure and analyze the particle configuration as well.

Bidisperse systems have been used in various granular studies. Usually, bidispersity is advantageous to prevent ordering with the crystalline configuration. Moreover, other structures, such as quasicrystals and DNA-like structures, can also be developed in bidisperse systems.^{2–4} To understand such complex structure formation processes, the effect of bidispersity on the disordering of

the particle configuration has to be revealed. In this study, we are going to focus on the magnet-particle system, in which the ordered configuration formed by a monodisperse system can be disturbed by introducing bidispersity. By using a binary mixture of two types of dipolar particles, a diverse array of crystalline or partially ordered structures can be generated.^{5–10} Under certain conditions, partial clustering¹¹ or relaxation after ultrafast quenching¹² can also be observed. While the characterization of various types of ordered structures is an interesting research topic, the current study aims to focus on the characterization of random structures through analyzing the distribution of the particle configuration.

The evaluation of the ordered configuration has extensively been studied in terms of melting (solid–liquid) transition.^{13–21} Particularly, in two-dimensional melting systems, the completely ordered (crystalline) structure is disrupted by the dislocation pairs of defects. Then, the completely disordered (random) structure is attained in the molten state. The hexatic state can be observed in between these ordered and disordered states. Various melting-related phenomena have been studied by using the concept of a two-dimensional melting model (e.g., Refs. 13 and 14). A more or less similar two-step melting-like behavior was found in a vibrated granular 2D layer.²² To characterize the hexatic phase, the bond orientational order correlation function has been used.¹⁴ In the molten state, the hexagonal order structure does not have a long range order. Thus, the bond orientational correlation function shows an exponential decay in space. Contrastively, the bond orientational correlation function becomes constant in the solid crystalline state. The bond orientational correlation function shows a power-law decay in hexatic states. Similarly, the radial distribution function has also been used to characterize the translational ordering degree of the particle configuration.

Recently, the solidification of the system with or without ordering has been studied also in terms of jamming transition.²³ Even biological systems show the jamming-like behavior.²⁴ In the context of jamming transition, the physical mechanism of solidification with a disordered structure has to be properly understood. Thus, a method to characterize the ordering/disordering in the jammed system should be developed. Particularly, when the number of particles is limited, simpler and more efficient ways of characterizing the order of the particle configuration are necessary. Although bidisperse systems have been used to mimic natural polydisperse systems, very weak bidispersity may not be adequate to attain a spatially homogeneously random state. Such weak bidispersity may cause spatially heterogeneous randomness, which could affect the physical behaviors of jammed systems composed of bidisperse particles. The current study aims to investigate the relationship between the degree of bidispersity and the homogeneity of the random structure.

Granular systems have been well studied as a typical example of macroscopic many-particle systems. In usual granular systems, friction due to particle–particle contact plays a major role to construct and keep the particle configuration. Recently, different types of granular materials consisting of magnetically repulsive particles have also been used to study non-contacting granular behaviors.^{25–27} For instance, two-dimensional magnet-particle systems have been utilized to study granular silo flow,^{25,26} impact drag force,²⁷ and slow compression mechanics.²⁸ Among magnetic particles, the physical contact can be suppressed and interactions can be mediated only by repulsive magnetic forces. Therefore, the particle

configurations can be easily rearranged. In addition, this non-contacting feature makes the measurement and analysis of particles easier. In the present study, therefore, we investigate the effect of bidispersity in a two-dimensional magnetic particle system in which there is no inter-particle contact.

In short, we study a two-dimensional system consisting of magnet particles that have repulsive interaction. This system can develop various ordered and disordered particle configurations by varying the degree of bidispersity. In this study, the number of particles is limited and the aspect ratio of the system is large. Therefore, we characterize the particle configuration by a simple method. A series of experiments are conducted, and a comprehensive analysis of the particle configuration is performed using Voronoi tessellation and global bond orientational order. Through the use of Voronoi cell area distributions, this study demonstrates that the moments of the distribution are effective and straightforward tools for characterizing the spatial homogeneity of disordered structures in the granular packing.

II. EXPERIMENTS

The experimental apparatus containing magnetic particles is a Hele–Shaw cell with transparent glass walls. Figure 1 shows the experimental apparatus: (a) front view and (b) schematic diagram. Two glass walls of 450 mm high, 340 mm wide, and 8 mm thick are used to construct the cell. Two glass plates are kept parallel with a gap width of 3.0–3.1 mm. The cell is vertically mounted on a universal testing machine (Shimadzu AGX).

Then, cylindrical magnets are dispersed into the cell. We use two types of NdFeB magnet particles. One is 5 mm in diameter and 3 mm in thickness and has a surface magnetic flux density of 4000 G (hereafter referred to as “large particles”). The other is 3 mm in diameter and 3 mm in thickness and has a surface magnetic flux density of 4100 G (hereafter referred to as “small particles”). All of these magnet particles are carefully placed so that the magnetic dipoles are perpendicular to the front and rear glass walls with identical

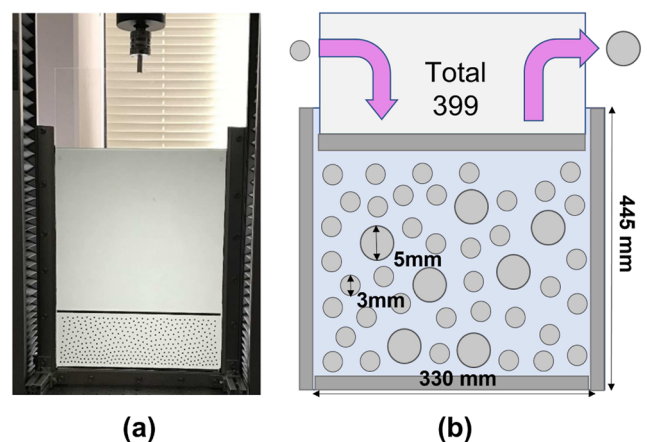


FIG. 1. Photograph and schematic diagram of the experimental equipment: (a) front view image and (b) schematic diagram with dimensions of the cell and magnet particles.

directions of the magnetic moment. Therefore, the magnet particles repel each other, without any physical contact. Rectangular NdFeB magnets are glued on the bottom and side walls to create a repulsive boundary condition. This configuration restricts the particle motions within a two-dimensional space. The magnetic particles are manually distributed in the cell to form a random initial structure. To effectively fill the cell with a large number of magnet particles as much as possible, the magnet-particle configurations are manually compressed. Then, the particles' initial configuration is determined by the repulsive force balance between particles. An acrylic plate (2 mm in thickness) is used as a piston to compress the particle system. Rectangular NdFeB magnets are glued on the bottom of the piston. The experimental system used in this investigation is akin to the system used in Ref. 28, which primarily examined the behavior of the compression force. However, this study concentrates on characterizing the order/disorder structure of particles within the compressed system.

In all experiments, the total number of particles is kept at 399. First, the experiment is performed with 399 large particles. It is difficult to add more particles without external loading due to limitations in the system size. The dimensions of the cell are limited by the frame dimensions of the universal testing machine we use in this study. We prepare the initial particle configurations with the above-mentioned procedure. The particle bed is then compressed by the piston at a constant speed of 1 mm s^{-1} . The compression is terminated when the compression force reaches 110 N, and the images of particle configurations are taken from the front of the cell by a still camera (Nikon, D7200). The acquired image size is 6000×4000 pixels. The spatial resolution of the acquired images is about $74\text{--}99 \mu\text{m}/\text{pixel}$. After unloading the particle system, a fixed number of large particles is replaced by an identical number of small particles. By this protocol, the ratio of the number of large particles and small particles can be varied while keeping the total number of particles constant. After replacing the particles, the magnets in the cell are stirred with a bamboo stick to make a random structure and to eliminate the memory of the particle configuration in the previous compression. Then, the system is compressed and the particle configuration is measured.

The aforementioned procedure is repeated until all particles are replaced by small particles. To check the reproducibility, two or more experimental runs are performed under each experimental condition. In the following data plots, all results of these experimental runs are shown in scatter plots. The mixing ratio R is defined by the ratio

$$R = \frac{N_{\text{small}}}{N_{\text{total}}}, \quad (1)$$

where N_{small} and $N_{\text{total}} = 399$ are the number of small particles and the total number of particles, respectively. The ImageJ software is used to locate the position of these particles. Figure 2 shows the example images before and after compression for the state of $R = 0.5$ (large 199 and small 200).

To stably compute the spatial correlation functions, such as the radial distribution function, the number of particles should be large and the system (boundary) should be more or less isotropic. However, in this study, we use a relatively small number of magnet particles confined in a thin (elongated) cell. Therefore, it is difficult to simply analyze the spatial correlation functions. Instead of spatial

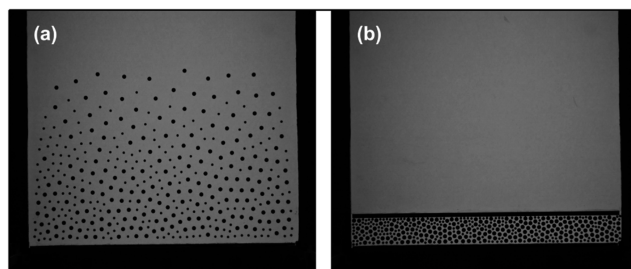


FIG. 2. Raw data of the experiment: 199 large particles and 200 small particles are distributed in the cell ($R = 0.5$). Photographs (a) before compression and (b) after compression are shown.

correlation functions, here we use a method characterizing global structure through the average of local characteristic quantities. The Voronoi tessellation and global bond orientational order (average of local bond orientational order) are more appropriate for extracting the geometrical characteristics of the assemblies.^{29–31}

An example of Voronoi tessellation is shown in Fig. 3 (pre-compression state of $R = 0.5$). In this figure, the blue dots represent the positions of the center of the magnet particles. The blue points are used as the reference generating points, and the plane coordinates are divided by line segments corresponding to the perpendicular bisectors of the neighbor generating points. In Fig. 3, the Voronoi cells near the walls diverge or have very large areas due to boundary effects. Therefore, the green rectangle in Fig. 3 that contains the topmost, bottommost, leftmost, and rightmost particles on the boundary is used to define the analysis area. We consider only the Voronoi cells whose entire shapes are in this rectangle as shown by pink colored cells in Fig. 3.

Using the generating points, the global bond orientational order parameter of the configuration can also be defined as¹⁷

$$\langle \Psi_6 \rangle = \left\langle \left| \frac{1}{n} \sum_{j=1}^n e^{i6\theta_{i,j}} \right| \right\rangle, \quad (2)$$

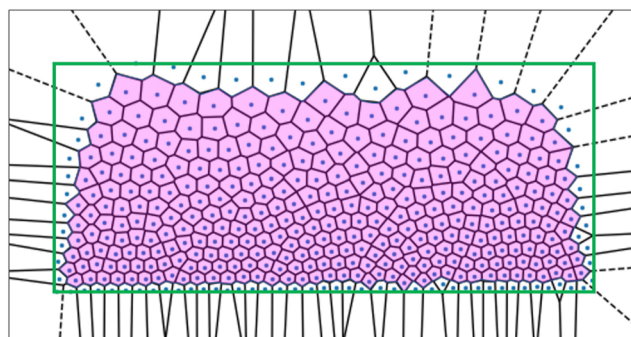


FIG. 3. An example of Voronoi tessellation based on the particle positions ($R = 0.5$, before compression). The blue dots represent the center of the particle, and the black lines represent the Voronoi partitions. Only filled (pink) Voronoi cells are analyzed.

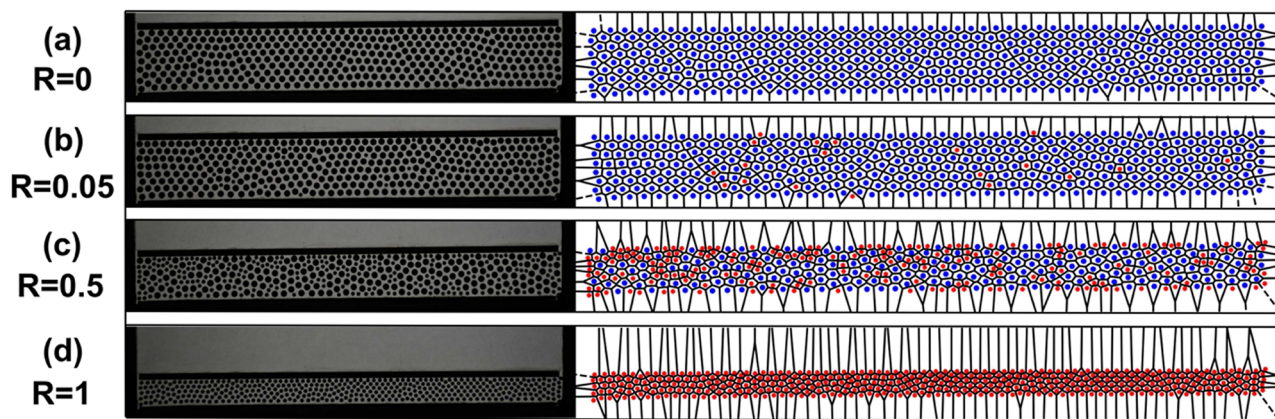


FIG. 4. Particle configurations of the compressed magnet-particle systems with various mixing ratios. The left column shows the raw data, and the right column shows the corresponding Voronoi diagrams. The blue and red dots represent the positions of large and small particles, respectively. (a) $R = 0$, (b) $R = 0.05$, (c) $R = 0.5$, and (d) $R = 1$. When $R = 0$ and 1, the height of the compressed particle configuration comprises only about nine and five rows of particles, respectively. Thus, many particles are affected by boundary walls.

where n represents the number of neighbors of i th particle, θ_{ij} is the angle between the horizontal axis and the bond linking i th particle and j th neighbor, and $\langle \cdot \rangle_i$ means the average of all particles. $\langle \Psi_6 \rangle$ becomes unity when the particle configuration obeys a completely ordered triangular (hexagonal) lattice structure. Note that the value of $\langle \Psi_6 \rangle$ decreases upon the introduction of randomness or specific types of crystalline structure in the system.

III. RESULTS

As shown in Figs. 2(a) and 3, the particle configuration before the compression is not uniform due to the effect of gravity. Because we would like to focus on the effect of bidispersity, we analyze the configurations after the compression and discuss the dependence on R . Raw images of particle configurations for $R = 0$, $R = 0.05$, $R = 0.5$, and $R = 1$ of the compressed states (110 N compression force) are shown in the left column of Fig. 4. When $R = 0$ [Fig. 4(a)], the particles are arranged in an ordered structure of a hexagonal array. At $R = 0.05$ [Fig. 4(b)], where there are a few small particles

mixed in the system, the ordered arrangement of the particles is slightly disrupted compared to the state of $R = 0$. In addition, the ratio of non-hexagonal arrangement increases. At $R = 0.5$ [Fig. 4(c)], where the numbers of large and small particles are almost identical, the particle configuration shows a disordered arrangement. At $R = 1$ [Fig. 4(d)], where all particles are small, the particle configuration order is recovered, and the arrangement is again almost hexagonal. However, the degree of ordering is smaller than the $R = 0$ state because the small size particles have relatively greater individual variation in the magnitude of the magnetic dipole moment. The individual variation of magnetic moment results in effective polydispersity. Furthermore, since the small-particle system is significantly compressed and many particles are next to the walls, the boundary effect (including friction with the walls) is also enhanced. Specifically, the height of the compressed particle configuration reduces to only five layers of particles when $R = 1$. Therefore, many particles are affected by boundary walls.

The Voronoi diagrams for $R = 0$, $R = 0.05$, 0.5, and 1 are shown in the right column of Fig. 4. At $R = 0$, the Voronoi cells are basically uniform in size. In addition, most of the Voronoi cells are hexagonal. At $R = 0.05$, some Voronoi cells are small. In addition, the number

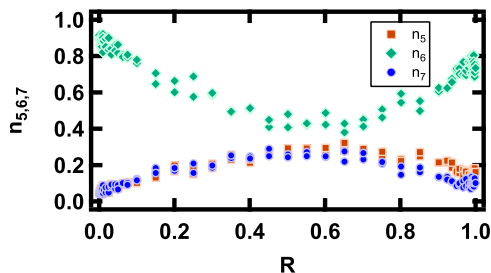


FIG. 5. The mixing ratio dependence of the number ratios of pentagons, hexagons, and heptagons of Voronoi cells, normalized to the total number of pentagons, hexagons, and heptagons. The horizontal axis shows the mixing ratio R , and the vertical axis shows the ratios of pentagons n_5 , hexagons n_6 , and heptagons n_7 .

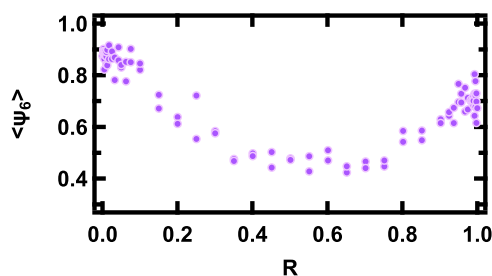


FIG. 6. $\langle \Psi_6 \rangle$ is plotted as a function of the mixing ratio R . The qualitative behavior of $\langle \Psi_6 \rangle$ is very similar to n_6 shown in Fig. 5.

of non-hexagonal Voronoi cells seems to increase. At $R = 0.5$, the Voronoi cells have various areas, and there are many non-hexagonal cells. At $R = 1$, the particles' arrangement recovers the ordering. The number of hexagonal Voronoi cells also increases in this state.

To characterize the observed features, we examine the fraction of hexagonal Voronoi cells with respect to the mixing ratio, R . The number ratios of pentagonal, hexagonal, and heptagonal Voronoi cells to the total number of the Voronoi cells are defined as n_5 , n_6 , and n_7 , respectively. There are few Voronoi cells other than pentagonal, hexagonal, and heptagonal cells. Figure 5 shows the R dependence of n_5 , n_6 , and n_7 .

As shown in Fig. 5, n_6 is large when $R = 0$ and it decreases as R increases. Then, n_6 reaches the minimum at $R \approx 0.5$. After that, n_6 increases again as R increases. The difference in n_6 between

$R = 0$ and 1 states (both of which consist of identical size particles) indicates the relatively worse ordering in $R = 1$ than in $R = 0$. As mentioned above, this type of asymmetry in n_6 curves probably comes from the enhanced individual variation and boundary effects. As a consequence of this asymmetry, the curve exhibits slight distortion, making it difficult to clearly identify the minimum of n_6 exactly at $R = 0.5$. By considering the data scattering, we consider the minimum of n_6 is achieved at $R \approx 0.5$.

The ratios of pentagonal and heptagonal cells (n_5 and n_7) are very small at $R = 0$ and 1 (monodisperse states). As R deviates from 0 or 1, n_5 and n_7 increase and show the maximum values at $R \approx 0.5$. The shapes of n_5 and n_7 curves are quite similar, and they have clear anti-correlation to n_6 . This tendency suggests that the hexagonal ordered structure is disrupted by the defect characterized by the pair of pentagonal and heptagonal cells. In this sense, the disordering process constructed by bidispersity could be similar to the two-dimensional melting situation.

To further evaluate this tendency, the R dependence of $\langle \Psi_6 \rangle$ is measured and plotted in Fig. 6. As shown in Fig. 6, the behavior of $\langle \Psi_6(R) \rangle$ is similar to that of $n_6(R)$. This correspondence is natural since both $\langle \Psi_6 \rangle$ and n_6 characterize the global hexagonal degree. Actually, a similar trend of $\langle \Psi_6 \rangle$ behavior has been found in Fig. 7.3 of Ref. 10.

For characterizing the degree of ordering in more detail, the dependence of the area distribution of the Voronoi cells on R is examined. Let x be the Voronoi cell area. Figure 7 shows the histograms of the x distribution. It is shown that the average of x

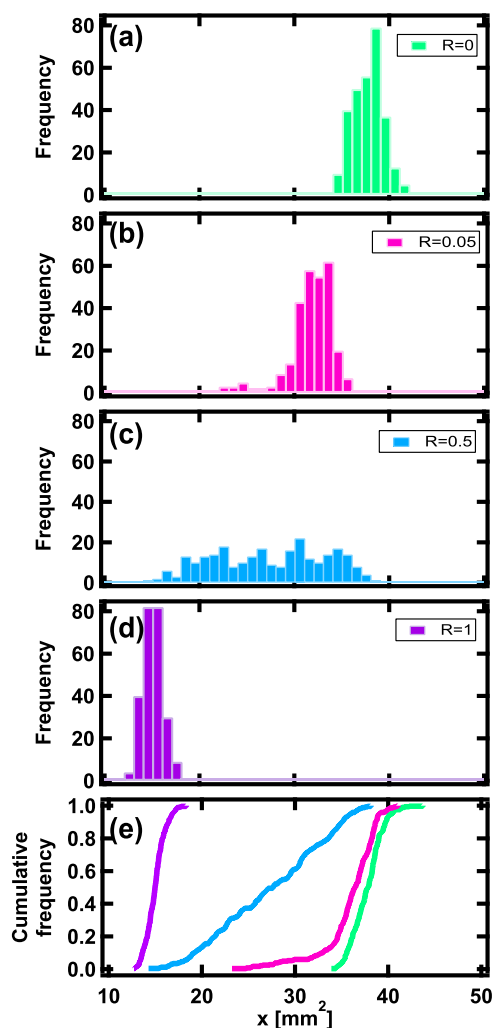


FIG. 7. The distributions of the area of Voronoi cells, where the horizontal axis is the Voronoi cell area and the vertical axis is the frequency. (a) $R = 0$, (b) $R = 0.05$, (c) $R = 0.5$, (d) $R = 1$. (e) Corresponding cumulative distribution curves. The color code used in (e) corresponds to the R values labeled in (a)–(d).

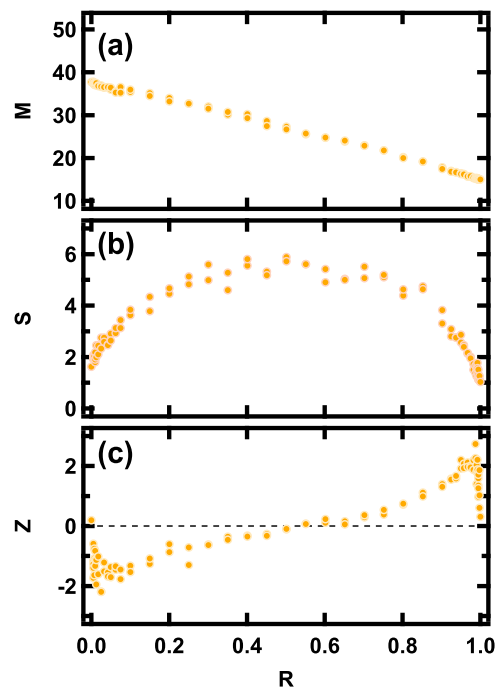


FIG. 8. Moments of the x (Voronoi cell area) distribution. (a) The mean area of Voronoi cell M , (b) the standard deviation S , and (c) the skewness Z as functions of the mixture ratio R are presented.

becomes smaller as R increases. At $R = 0$ [Fig. 7(a)], the x distribution is narrower and symmetric. At $R = 0.05$ [Fig. 7(b)], the area distribution shifts toward the smaller x range and becomes broader than the distribution at $R = 0$. Moreover, the asymmetry of the distribution is enhanced particularly due to the existence of small x ($\approx 25 \text{ mm}^2$) cells. This smaller x population represents the small particles contribution. At $R = 0.5$ [Fig. 7(c)], the distribution of x shifts further toward the smaller x range. The peak height is very small, and the distribution becomes extremely broad. However, the symmetry of the distribution is recovered in this state. At $R = 1$ [Fig. 7(d)], the distribution shifts to an even smaller range. However, the symmetry of the distribution is not disrupted because all the particles in this state are small. To clearly show the above-mentioned characteristics, the corresponding cumulative distribution curves are also shown in Fig. 7(e).

In order to characterize the distribution, we evaluate the mean M , standard deviation S , and skewness Z of the x distribution. Figure 8 shows the dependence of M , S , and Z of the Voronoi cell area on R . Let

$$m_k = \frac{1}{N} \sum (x - M)^k \quad (3)$$

be the k th moment of the distribution. Then, the standard deviation is written as

$$S = m_2^{1/2}. \quad (4)$$

In addition, the skewness is written as

$$Z = \frac{m_3}{m_2^{3/2}}. \quad (5)$$

Figure 8(a) shows that M decreases almost linearly with increasing R . In Fig. 9(a), the average areas of the cells of pentagons, hexagons, and heptagons are shown. As shown in Fig. 9(a), the M of a hexagon is close to the M of a heptagon when $R < 0.5$. In

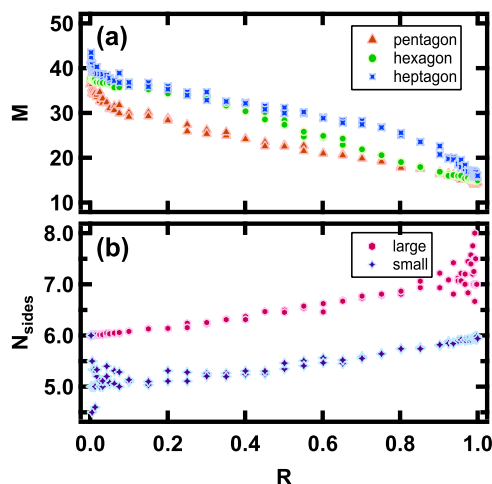


FIG. 9. Properties of polygons of large and small particles. (a) The mean area of Voronoi cell M and (b) the average number of sides of Voronoi cells N_{sides} around large and small particles are plotted as a function of mixing ratio R .

addition, when $R > 0.5$, the M of a hexagon approaches the M of a pentagon. This means that the small particles tend to form smaller pentagons and the large particles tend to form larger heptagons. To clearly show this trend, the relation between the average number of sides (neighbor particles) N_{sides} of the Voronoi cells around large or small particles and the mixing ratio R is shown in Fig. 9. By adding large (or small) particles, a heptagon (or a pentagon) is formed around the added particle. By this disturbance, some major small (or large) particles' Voronoi cell becomes a pentagon (or a heptagon). The two-dimensional hexagonal order is disrupted by introducing bidispersity in this manner.

In Fig. 8(b), S has a small value at $R = 0$ and increases as R increases. Then, S shows the maximum value around $R = 0.5$. In the range of $R > 0.5$, S decreases as R increases. The shape of $S(R)$ is qualitatively similar to $n_{5,7}$ curves and almost symmetric. If S is normalized to M , the S/M curve shows a slightly asymmetric feature like $n_{5,7}$ curves.

In Fig. 8(c), one can confirm that Z is ~ 0 at $R = 0$. Then, the value of Z rapidly decreases with increasing R until $R \approx 0.05$, where Z has a negative peak (minimum) value. The negative values of Z indicate that the distribution is asymmetric due to the tail in the small x range. This asymmetry of the distribution characterized by Z is enhanced when $\sim 5\%$ of small particles are present in the system. Then, in the range of $0.05 \lesssim R \lesssim 0.95$, Z increases as R increases. At $R = 0.5$, Z becomes almost 0. This indicates that x is symmetrically distributed at $R = 0.5$. Z shows the maximum value around $R = 0.95$. This implies that the presence of a small number ($\approx 5\%$) of a large Voronoi cell yields the asymmetry in the x distribution, as in the case of $R = 0.05$.

IV. DISCUSSION

First, we compare our results with a previous study¹ that used photoelastic particles to investigate the relationship between the mixing ratio and the orientational order of the force chain structure in a two-dimensional granular system. In this previous study, the degree of orientational order shows the maximum when $R = 0$. Then, as R increases, the value of the orientational order decreases until around $R = 0.1$. However, the value of the orientational order does not vary in the range of $0.1 \leq R \leq 0.9$. From $R = 0.9$ to $R = 1$, the value of the orientational order increases with increasing R . At $R = 1$, the value of the orientational order again shows the maximum value. From these results, the previous study concluded that about 10% bidispersity is sufficient to achieve the spatially homogeneous random structure. However, the current experimental results present a different scenario to develop a random structure by bidispersity. The characteristic feature found in this study is the continuous decrease in $n_6(R)$ and $\langle \Psi_6(R) \rangle$ from $R = 0$ to $R = 0.5$. We do not observe a clear plateau behavior in the range of $0.1 \leq R \leq 0.9$. In addition, in Fig. 8(a), $M(R)$ linearly decreases from $R = 0$ to $R = 1$. In Fig. 8(b), S continuously increases from $R = 0$ to $R = 0.5$. Regarding the skewness behavior, $Z(R)$ shows a peak value at $R \approx 0.05$ as shown in Fig. 8(d). However, $Z(R)$ continuously varies in $R \geq 0.05$. The symmetric x distribution characterized by $Z \approx 0$ is achieved at $R \approx 0.5$, and the Z value varies symmetrically around $R \approx 0.5$. Thus, in the present magnet-particle system, we consider that the degree of the configurational order continuously varies all the way from $R = 0$ to $R = 0.5$. Perhaps, the

best mixing ratio ($R \approx 0.5$ in this study) might depend on the size ratio of large and small particles. Although we guess $R \approx 0.5$ is appropriate for a realistic size-ratio range (e.g., less than factor 2 difference), the size ratio dependence of the best R value is a future problem.

The current result suggests that $R \approx 0.5$ is an ideal mixing of large and small particles to achieve the symmetric random distribution. As revealed by the previous study,¹ 10% bidispersity is sufficient to make random structures in terms of the force chain orientational order. Our study reveals that the skewness suggests that the ordered structure is more or less disrupted when $R \approx 5\%$. This significant skewness can be attributed to the contribution of small particles to the disordering of the particle configuration. By considering the Voronoi-cell-area distribution and global bond orientational order, we find the maximum disorder is attained at $R \approx 0.5$. However, note that we do not measure the force chain network. It is difficult to define force chain structure in the magnetic particle system. Thus, we characterize the particle configuration directly. In the current study, the asymmetry of the Voronoi-cell-area distribution can surely be confirmed at a 10% bidisperse state. To eliminate the asymmetry, $\approx 50\%$ bidispersity is better. If one aims to mimic natural disorder systems in granular experiments/simulations using bidispersity, using only 10% bidispersity may not suffice. This is due to the asymmetric distribution characterized by skewness, which can affect the macroscopic behaviors of the system. To eliminate such artificial effects, using a bidispersity of $\sim 50\%$ is better. Furthermore, the ratios among pentagonal, hexagonal, and heptagonal structures also indicate that $\approx 50\%$ bidispersity ($R \approx 0.5$) is better to form a random structure. However, both the interparticle contact force and analysis methods are different between the previous work¹ and the current study. The effective force chain structure might be defined in the magnetic system as well. Quantitative analysis of the force balance in the magnet-particles system might reveal the details of the particle configuration. Further systematic experiments are necessary

to clarify details about the effect of physical contact among particles. This is an important future work.

Usually, the spatial correlation of the bond orientational order $G_6(|\mathbf{r} - \mathbf{r}'|) = \langle \exp(6i[\theta(\mathbf{r}) - \theta(\mathbf{r}')]) \rangle$, where \mathbf{r} and \mathbf{r}' are the position vectors of the particles and θ denotes the angle to the horizontal axis, is also used to characterize the ordered degree; this value does not show a clear R dependent variation in the current system. $G_6(r)$ data scatter, and it is difficult to clearly confirm the $r (= |\mathbf{r} - \mathbf{r}'|)$ -dependent decaying behavior. Only the global bond order parameter $\langle \Psi_6 \rangle$ can properly characterize the system in this study. This difficulty comes from the less number of particles and very compressed (thin) cell's anisotropic effects, including boundary walls. Moreover, we realize that the systematic analysis of radial distribution function is also difficult due to the same reason. Namely, although the number of particles in the current experimental system is small and the system is thin to directly evaluate through spatial correlations, such as $G_6(r)$ and the radial distribution function, the statistics of Voronoi cells and $\langle \Psi_6 \rangle$ allow us to characterize the global degree of the ordering in a two-dimensional bidisperse system. The shape and area distributions of the Voronoi cells can characterize the state of randomness.

Based on Figs. 5, 6, and 8(b), it can be observed that n_6 , $\langle \Psi_6 \rangle$, and S exhibit qualitatively similar trends. To quantitatively characterize this relationship, direct correlations among n_6 , $\langle \Psi_6 \rangle$, and S are shown in Fig. 10. One can confirm the good correlations. The correlation coefficients are 0.97 and -0.81 for $\langle \Psi_6 \rangle$ vs n_6 and S vs n_6 , respectively. Thus, we consider that any of them can similarly characterize the disorder degree.

In the current system, we do not have any thermal effect, such as random motion of particles. To mimic the two-dimensional melting by this system, a certain analog of thermal fluctuation should be added to the system. Perhaps, mechanical vibrations can be used as a source of such fluctuation.¹⁵ Then, we can consider the melting of the ordered structure by the thermal effect. The temperature is directly measurable by the random motion of the particles in this system. This is the advantage of a macroscopic granular system. The pressure is certainly measurable by the confining piston force. Then, the equation of state of the magnetic particle system can be built through this kind of experiment. Finally, the slow compression force of the monodisperse magnet-particle system was reported by Modesto *et al.*²⁸ The effect of bidispersity on the compression force would also be an interesting future problem.

Moreover, our analysis is limited to the highly compressed state achieved with the 110 N compression force. It has been reported in Ref. 28 that the compression force nonlinearly increases as the compression proceeds and exhibits hysteresis. The relationship between the particle configuration order and compression force is an intriguing topic for further exploration. By increasing the compression force, the effect of gravity on the particle configuration order would be gradually reduced. Investigating the structural development of the compressed magnet system in more detail is also an interesting future research problem. Additionally, the effect of bidispersity on compression force can be examined by comparing our experimental results with the previous study. To eliminate the effect of gravity, a horizontal setup can be employed, which is currently being pursued as an extension of our experimental setup. It should be noted that the gravity effect is negligible even in the current vertical setup as long as the granular layer is sufficiently compressed. If the hor-

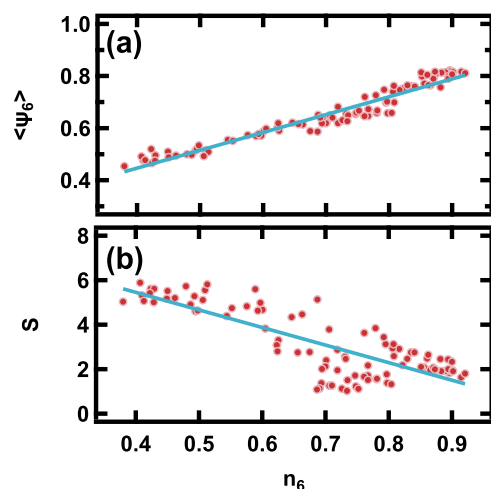


FIG. 10. Correlations between (a) $\langle \Psi_6 \rangle$ vs n_6 and (b) S vs n_6 . In both panels, clear correlations can be confirmed as shown by the linear fitting lines. The correlation coefficients are 0.97 and -0.81 for (a) and (b), respectively.

izontal setup is used, the gravity effect becomes negligible from the initial state prior to the compression. In addition, we plan to perform corresponding numerical simulations to investigate a wider range of parameter values. The results of these investigations will be reported in future publications.

V. CONCLUSION

The effect of bidispersity on the ordered particle configuration is experimentally studied in a two-dimensional granular layer consisting of repulsive magnets. Voronoi tessellation is used to investigate the R (mixing ratio) dependence of the degree of ordering through the hexagonal ratio of Voronoi cells n_6 , the global bond orientational order parameter $\langle \Psi_6 \rangle$, and the Voronoi cell area distribution. As a result, n_6 and S (standard deviation of area distribution) show a continuous peak around $R \approx 0.5$. The value of Z (skewness of area distribution) shows the peak at $R \approx 0.05$, and Z becomes almost 0 at $R \approx 0.5$. These results indicate that the random structure without any asymmetric distribution is achieved at $R \approx 0.5$. This is in contrast to the results of a previous study, which showed that the value of the orientational order of the force chain structure does not change in the range of $R = 0.1$ – 0.9 . According to the current result, a truly equal number bidispersity is favorable to attain the ideal random structure by using bidispersity. The system we use in this study is different from a usual granular system. Therefore, further studies with various setups are necessary to discuss general features to achieve an ideally random granular structure.

ACKNOWLEDGMENTS

This work was partially supported by JSPS KAKENHI Grant Nos. 18H03679 and 23H04134. S.D. acknowledges F.R.S.-FNRS for the financial support as a senior research associate. Y.D.S. acknowledges FAP-DF Project No. 00193-00001155/2021-40 for the financial support.

AUTHOR DECLARATIONS

Conflict of Interest

The authors have no conflicts to disclose.

Author Contributions

K. Tsuchikusa: Data curation (lead); Investigation (lead); Writing – original draft (equal); Writing – review & editing (equal). **K. Yamamoto:** Investigation (supporting); Supervision (supporting); Writing – review & editing (supporting). **M. Katsura:** Investigation (supporting); Supervision (supporting); Writing – review & editing (supporting). **C. T. de Paula:** Conceptualization (equal); Writing – review & editing (equal). **J. A. C. Modesto:** Conceptualization (equal); Writing – review & editing (equal). **S. Dorbolo:** Conceptualization (equal); Writing – review & editing (equal). **F. Pacheco-Vázquez:** Conceptualization (equal); Writing – review & editing (equal). **Y. D. Sobral:** Conceptualization (equal); Writing – review & editing (equal). **H. Katsuragi:** Conceptualization (equal); Funding acquisition (lead); Investigation (supporting); Supervision

(lead); Writing – original draft (supporting); Writing – review & editing (lead).

DATA AVAILABILITY

The data that support the findings of this study are available from the corresponding author upon reasonable request.

REFERENCES

- 1 N. Iikawa, M. M. Bandi, and H. Katsuragi, “Sensitivity of granular force chain orientation to disorder-induced metastable relaxation,” *Phys. Rev. Lett.* **116**, 128001 (2016).
- 2 A. Reinhardt, J. S. Schreck, F. Romano, and J. P. K. Doye, “Self-assembly of two-dimensional binary quasicrystals: A possible route to a DNA quasicrystal,” *J. Phys.: Condens. Matter* **29**, 014006 (2017); arXiv:1607.06626.
- 3 E. Fayen, A. Jagannathan, G. Foffi, and F. Smalenburg, “Infinite-pressure phase diagram of binary mixtures of (non)additive hard disks,” *J. Chem. Phys.* **152**, 204901 (2020); arXiv:2003.08889.
- 4 E. Fayen, M. Impéror-Clerc, L. Filion, G. Foffi, and F. Smalenburg, “Self-assembly of dodecagonal and octagonal quasicrystals in hard spheres on a plane,” *Soft Matter* **19**, 2654–2663 (2023).
- 5 L. Assoud, R. Messina, and H. Löwen, “Stable crystalline lattices in two-dimensional binary mixtures of dipolar particles,” *Europhys. Lett.* **80**, 48001 (2007); arXiv:0706.2311.
- 6 R. Messina and S. Aljawhari, “Crystallization of binary mixtures of similar dipole moments in two dimensions: A Monte Carlo study,” *Europhys. Lett.* **115**, 28005 (2016).
- 7 F. Ebert, P. Keim, and G. Maret, “Local crystalline order in a 2D colloidal glass former,” *Eur. Phys. J. E* **26**, 161–168 (2008).
- 8 J. Fornleitner, F. Lo Verso, G. Kahl, and C. N. Likos, “Genetic algorithms predict formation of exotic ordered configurations for two-component dipolar monolayers,” *Soft Matter* **4**, 480–484 (2008).
- 9 J. Fornleitner, F. Lo Verso, G. Kahl, and C. N. Likos, “Ordering in two-dimensional dipolar mixtures,” *Langmuir* **25**, 7836–7846 (2009).
- 10 J. Schockmel, “Self-organization of a monolayer of magnetized beads,” Ph.D. thesis, Université de Liège, 2019.
- 11 F. Ebert, G. Maret, and P. Keim, “Partial clustering prevents global crystallization in a binary 2D colloidal glass former,” *Eur. Phys. J. E* **29**, 311–318 (2009); arXiv:0903.2812.
- 12 L. Assoud, F. Ebert, P. Keim, R. Messina, G. Maret, and H. Löwen, “Ultrafast quenching of binary colloidal suspensions in an external magnetic field,” *Phys. Rev. Lett.* **102**, 238301 (2009); arXiv:0811.1498.
- 13 K. J. Strandburg, “Two-dimensional melting,” *Rev. Mod. Phys.* **60**, 161–207 (1988).
- 14 U. Gasser, C. Eisenmann, G. Maret, and P. Keim, “Melting of crystals in two dimensions,” *ChemPhysChem* **11**, 963–970 (2010).
- 15 J. Schockmel, E. Mersch, N. Vandewalle, and G. Lumay, “Melting of a confined monolayer of magnetized beads,” *Phys. Rev. E* **87**, 062201 (2013).
- 16 R. Messina, S. Aljawhari, L. Bécu, J. Schockmel, G. Lumay, and N. Vandewalle, “Quantitatively mimicking wet colloidal suspensions with dry granular media,” *Sci. Rep.* **5**, 10348 (2015).
- 17 J. Schockmel, N. Vandewalle, E. Opsomer, and G. Lumay, “Frustrated crystallization of a monolayer of magnetized beads under geometrical confinement,” *Phys. Rev. E* **95**, 062120 (2017).
- 18 E. Opsomer, S. Merminod, J. Schockmel, N. Vandewalle, M. Berhanu, and E. Falcon, “Patterns in magnetic granular media at the crossover from two to three dimensions,” *Phys. Rev. E* **102**, 042907 (2020).
- 19 K. Zahn, R. Lenke, and G. Maret, “Two-stage melting of paramagnetic colloidal crystals in two dimensions,” *Phys. Rev. Lett.* **82**, 2721–2724 (1999).
- 20 N. Gribova, A. Arnold, T. Schilling, and C. Holm, “How close to two dimensions does a Lennard-Jones system need to be to produce a hexatic phase?,” *J. Chem. Phys.* **135**, 054514 (2011); arXiv:1104.0611.

- ²¹Y. Komatsu and H. Tanaka, “Roles of energy dissipation in a liquid-solid transition of out-of-equilibrium systems,” *Phys. Rev. X* **5**, 031025 (2015); [arXiv:1509.03435](#).
- ²²P. M. Reis, R. A. Ingale, and M. D. Shattuck, “Crystallization of a quasi-two-dimensional granular fluid,” *Phys. Rev. Lett.* **96**, 258001 (2006); [arXiv:cond-mat/0603408](#).
- ²³R. P. Behringer and B. Chakraborty, “The physics of jamming for granular materials: A review,” *Rep. Prog. Phys.* **82**, 012601 (2018).
- ²⁴D. Bi, X. Yang, M. C. Marchetti, and M. L. Manning, “Motility-driven glass and jamming transitions in biological tissues,” *Phys. Rev. X* **6**, 021011 (2016); [arXiv:1509.06578](#).
- ²⁵G. Lumay, J. Schockmel, D. Hernández-Enríquez, S. Dorbolo, N. Vandewalle, and F. Pacheco-Vázquez, “Flow of magnetic repelling grains in a two-dimensional silo,” *Pap. Phys.* **7**, 070013 (2015).
- ²⁶D. Hernández-Enríquez, G. Lumay, and F. Pacheco-Vázquez, “Discharge of repulsive grains from a silo: Experiments and simulations,” *EPJ Web Conf.* **140**, 03089 (2017).
- ²⁷Y. Y. Escobar-Ortega, S. Hidalgo-Caballero, J. O. Marston, and F. Pacheco-Vázquez, “The viscoelastic-like response of a repulsive granular medium during projectile impact and penetration,” *J. Non-Newtonian Fluid Mech.* **280**, 104295 (2020).
- ²⁸J. A. C. Modesto, S. Dorbolo, H. Katsuragi, F. Pacheco-Vázquez, and Y. D. Sobral, “Experimental and numerical investigation of the compression and expansion of a granular bed of repelling magnetic disks,” *Granular Matter* **24**, 105 (2022).
- ²⁹Q. Yu, A. S. Ahmad, K. Stähl, X. D. Wang, Y. Su, K. Glazyrin, H. P. Liermann, H. Franz, Q. P. Cao, D. X. Zhang, and J. Z. Jiang, “Pressure-induced structural change in liquid GaIn eutectic alloy,” *Sci. Rep.* **7**, 1139 (2017).
- ³⁰J. L. Finney, “Modelling the structures of amorphous metals and alloys,” *Nature* **266**, 309–314 (1977).
- ³¹J. L. Finney and J. D. Bernal, “Random packings and the structure of simple liquids. I. The geometry of random close packing,” *Proc. R. Soc. London, Ser. A* **319**, 479–493 (1970).